FUNCTIONALIZED SURFACES: SILICA STRUCTURE AND METAL ION ADSORPTION BEHAVIOR

IAN P. BLITZ, JONATHAN P. BLITZ*, VLADIMIR M. GUN'KO[1], DANIEL J. SHEERAN
Eastern Illinois University, Charleston, IL 61920 USA
[1]Institute of Surface Chemistry 03164 Kiev, Ukraine

Abstract. Two silica gels with different sized mesopores and one nanoparticulate fumed silica, were modified with amino- and mercapto-functional silanes. One aminofunctional silane used was monofunctional preventing polymerization, the other trifunctional which permits surface polymerization. Structural and textural characteristics of these silicas before and after surface modification were probed using N_2 adsorption. The trifunctional aminosilane resulted in a material with less porosity than the monofunctional silane, which affected adsorption capacity of tested Cu(II) and Pb(II) from aqueous solution. Surface functionalization with the mercaptofunctional silane resulted in the smallest loss in porosity. A narrow pore size results in a more favorable ΔG_{ads}, but a larger pore size insures greater access of surface groups to adsorbed ions resulting in enhanced adsorption capacity. A comparison of the adsorption behavior of amino and mercapto groups for Cu(II) and Pb(II) shows that Cu(II) adsorbs to a greater extent on amino-functionalized than mercapto-functionalized surfaces. Pb(II) adsorption is not as greatly affected by the type of surface functionalization under the conditions studied.

Keywords: silica, organosilane, metal adsorption, isotherms, surface modification

1. Introduction

1.1. GENERAL OVERVIEW

An abundance of clean, uncontaminated water is a fundamental requirement for human life and environmental protection. As a result of various technological

*To whom correspondence should be addressed. J. P. Blitz, Eastern Illinois University, Charleston, IL 61920 USA E-mail jpblitz@eiu.edu

J.P. Blitz and V.M. Gun'ko (eds.), Surface Chemistry in Biomedical and Environmental Science, 337–348.

activities in the past century including mining, nuclear energy and the burning of fossil fuels, metal ions such as Sr^{2+}, Cs^{+}, Hg^{2+}, Cu^{2+}, Pb^{2+} and Cd^{2+} have been released into the environment at unprecedented levels. Considerable effort has gone into searching for the best ways to rid aqueous solutions of these unwanted solutes.[1,2]

Materials that contain functional groups to complex dissolved metal ions in aqueous solutions can be very effective. The use of an inorganic matrix, onto which a variety of functional groups can be chemically immobilized, has signficant advantages over conventional organic/polymeric supports. These advantages include a high surface area to enhance adsorption capacity, and greater physical and chemical robustness to withstand a variety of harsh environments. Whereas clays are a natural form of support to use,[3,4] various synthetic forms of silica provide a greater ability to vary the structure of these materials to optimize adsorption properties.

Highly structured mesoporous silicas using a surfactant template provide a well characterized, ultra-high surface area material.[5] In this volume Jaroniec provides an excellent summary of various novel materials based on this chemistry for Hg^{2+} adsorption. In this report we discuss results from a recent study utilizing two types of silica gels and a nanoparticulate fumed silica, all surface modified with complexing functional groups, for the adsorption of Cu^{2+} and Pb^{2+}.

1.2. BRIEF SCIENTIFIC BACKGROUND

Leyden and coworkers[6] were the first to use organosilane-modified silica surfaces to chelate metal ions, as an analytical preconcentration tool for subsequent analysis by EDXRF. While much has been learned since this time, fundamental questions remain concerning important factors which affect the metal adsorption behavior on these types of materials. The role of three main factors will be investigated in this work:

1. how the potential for the organosilane to form a cross-linked polymeric type of modified surface affects adsorption;
2. how the structural/textural characteristics of the modified surface affects metal adsorption behavior;
3. how the chemical functionality (mercapto versus amino) of the organosilane-modified surface affects adsorption of Cu^{2+} and Pb^{2+} from aqueous solution.

The first two factors above are linked since cross-linking on the surface and inside the pores of a silica gel can signficantly affect porosity. This cross-linking is varied by using organosilanes with either one or three hydrolyzable

groups for surface modification. Organosilanes with one hydrolyzable group are unable to crosslink;

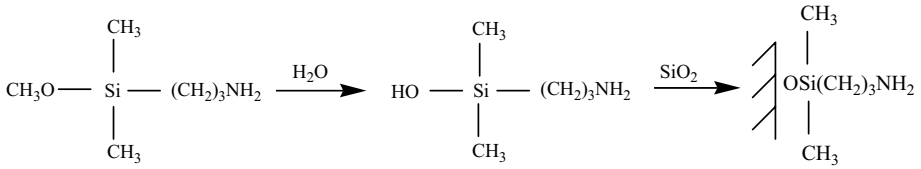

whereas organosilanes with three hydrolyzable groups are able to form polymeric phases on the surface as depicted below.

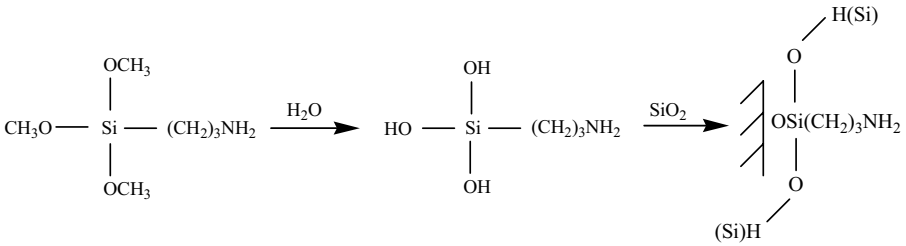

Porosity and pore size distributions, both before and after surface modification, are analyzed from N_2 adsorption data. Both capacity as well as adsorption free energies are obtained from metal ion adsorption isotherms from aqueous solution as described in the experimental section.

2. Experimental

2.1. MATERIALS

The nanoparticulate fumed silica Cab-O-Sil HS5 was provided from the Cabot Corporation, silica gels HP39 and 200DF were provided by Crosfield, and used as received. The organosilanes 3-aminopropyltriethoxysilane, 3-aminopropyldimethylmethoxysilane, and 3-mercaptopropyltrimethoxysilane were purchased from Gelest and used as received. All aqueous solutions were made from Millipore® water. Standard Cu^{2+} solutions were prepared using Cu wire dissolved in HNO_3 (pH subsequently adjusted to 5.0 by dropwise addition of NaOH), and Pb^{2+} solutions using primary standard $PbNO_3$ with a natural solution pH very close to 5.

2.2. METHODS

2.2.1. Materials synthesis

Four grams of silica was reacted with 20 mmoles of organosilane in 200 mL of refluxing toluene for a minimum of 2 hours. The slurry was filtered and washed with toluene, then dried at 150°C in vacuum for 2 hours. Reactions with the mercaptosilane were carried out in the presence of 100 μl of n-butylamine catalyst. The trialkoxysilane-modified silicas were resuspended in millipore water for 30 minutes, then once again dried in vacuum at 150°C to facilitate cross-linking. The extent of aminosilane reaction was determined by combustion analysis using a CE440 Microanalyzer (±0.06%), and mercaptosilane reaction using S analysis by ICP with a Perkin-Elmer 2000DV. Surface modification was verified by FTIR spectroscopy as characteristic NH_2 and SH functional group frequencies are readily detected.

2.2.2. Nitrogen adsorption data collection and analysis

Approximately 0.3 g of sample was outgassed at 110°C prior to analysis. Nitrogen adsorption-desorption isotherms were recorded at 77.35 K using a Micromeritics ASAP 2010 adsorption analyzer at $p/p_0 > 10^{-6} - 10^{-5}$, where p and p_0 denote the equilibrium pressure and saturation pressure of nitrogen at 77.35 K, respectively.

Pore size distributions (PSDs) (differential PSD $f_V(R_p) \sim dV_p/dR$) of the studied adsorbents were calculated using modified overall adsorption equation in the form proposed by Nguyen and Do (ND method)[7,8] for slitshaped pores of carbons and modified for other materials with cylindrical pores and pores as gaps between spherical particles.[9-16] The nitrogen desorption data were utilized to compute the $f_V(R_p)$ distribution functions using a modified regularization procedure[17] under non-negativity condition ($f_V(R_p) \geq 0$ at any R_p) with a fixed regularization parameter $\alpha = 0.01$.

The $f_V(R_p)$ functions linked to pore volume can be transformed to the $f_S(R_p)$ distribution functions with respect to surface area using the corresponding pore models

$$f_S(R_p) = \frac{w}{R_p}\left(f_V(R_p) - \frac{V_p}{R_p}\right) \tag{1}$$

where $w = 1$, 2, 3, and 1.36 for slitlike, cylindrical, spherical pores and gaps between spherical particles packed in the cubic lattice. The $f_V(R_p)$ and $f_S(R_p)$ functions were used to calculate contributions of nanopores (V_{nano} and S_{nano} at the pore radius $R_p < 1$ nm), mesopores (V_{mes} and S_{mes} at 1 nm $\leq R_p \leq$ 25 nm), and macropores (V_{mac} and S_{mac} at $R_p > 25$ nm) to the total pore volume and the

specific surface area (Table 2). The values of S_{nano}, S_{mes}, and S_{mac} were corrected such that $S_{nano} + S_{mes} + S_{mac} = S_{BET}$.

For a pictorial presentation of the pore size distributions, the $f_V(R_p)$ functions were re-calculated to incremental PSDs (IPSDs)

$$\Phi_V(R_{p,i}) = 0.5(f_V(R_{p,i}) + f_V(R_{p,i-1}))(R_{p,i} - R_{p,i-1}) . \quad (2)$$

2.2.3. Metal ion adsorption data collection and analysis

Various concentrations (10.00 mL) of Cu^{2+} or Pb^{2+} solutions were exposed to 0.0250 g of silica in sealed conical flasks for 16 hours in a wrist action shaker. The slurries were centrifuged, solution aliquots then obtained and analyzed by atomic absorption (AA, Perkin-Elmer 2380). The extent of metal ion adsorption on silica was obtained by subtracting the amount of metal ion present in solution after adsorption from the amount of metal ion in the original solution.

To calculate the free energy distributions ($f(\Delta G)$) of ion adsorption, the Langmuir equation was used as the kernel of the Fredholm integral equation of the first kind

$$\Theta = \int \frac{z \exp(-\frac{\Delta G - \gamma}{R_g T})}{1 + z \exp(-\frac{\Delta G - \gamma}{R_g T})} f(\Delta G) d(-\Delta G) \quad (3)$$

where $\Theta = a/a_m$ is the relative adsorption, a_m is the monolayer capacity; $z = C_{ads}/C_{eq}$, and R_g is the gas constant. Eq. (3) was solved using the regularization procedure under non-negativity condition ($f(\Delta G) \geq 0$ at any ΔG) with a fixed regularization parameter $\alpha = 0.01$.

3. Results and Discussion

Results of the extent of surface modification reaction of the three silicas with the three organosilanes studied are shown in Table 1.

Table 1. Elemental analysis results of organosilane-modified silicas. APDMS = 3-aminopropyldimethylmethoxysilane; APTS = 3-aminopropyltriethoxysilane; MPTMS = 3-mercaptopropyltrimethoxysilane.

Organosilane	mmol N(S)/g Cab–O–Sil HS5	mmol N(S)/g Crosfield HP39	mmol N(S)/g Crosfield 200DF
APDMS	1.684	1.963	1.920
APTS	1.224	1.781	1.281
MPTMS	(0.823)	(1.101)	(1.319)

The extent of surface modification for both Cab-O-Sil and HP39 follows the trend APDMS > APTS > MPTMS. More MPTMS reacts with 200DF silica gel

than APTS, which may be explained by data below concerning the porosity of these silicas before and after surface modification. These three silicas were chosen for study because of their varying structural/textural characteristics, characterized by N_2 adsorption. As illustrated in Table 2 and Figures 1 and 2, the surface area and porosity of these silicas are quite different.

Table 2. Structural characteristics of silicas before surface modification.

Silica	S_{BET} (m^2/g)	S_{nano} (m^2/g)	S_{meso} (m^2/g)	S_{mac} (m^2/g)
HS5	326	152	129	45
HP39	467	125	272	70
200DF	540	208	312	20

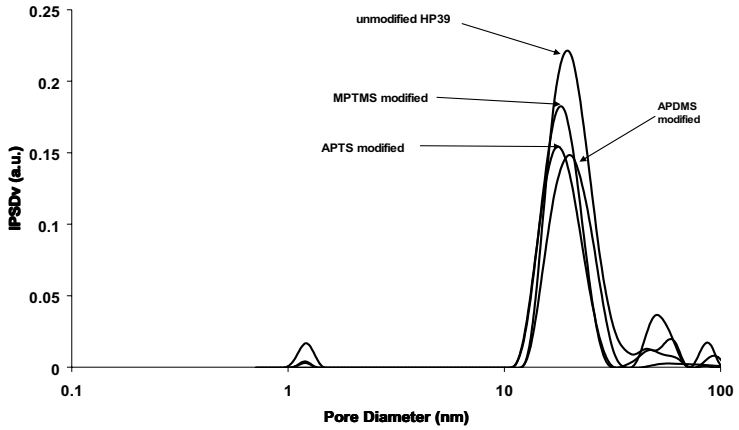

Figure 1. Incremental pore size distributions of HP39 before and after surface modification with APDMS, APTS, and MPTMS.

It is worth mentioning that the surface area of Cab-O-Sil fumed silica is derived from its very small particle size, and its porosity is determined by the arrangement of these primary particles into aggregates and larger agglomerates. Thus the surface area of this nanoparticulate fumed silica is subject to large changes dependent upon its physical environment and history. These effects are beyond the scope of this paper, but have been addressed in other contributions in this volume and elsewhere.[13,14,16] Effects of surface modification on porosity are thus addressed only for the silica gels.

It is not surprising that in all cases surface modification results in a reduction in pore volume. The average pore diameter of 20 nm for HP39 is unchanged as a result of modification by APDMS. However, reaction with trifunctional APTS or MPTMS results in a reduced average pore size of approximately 18 nm, indicating some surface polymerization may result in a ~10% reduction in pore diameter.

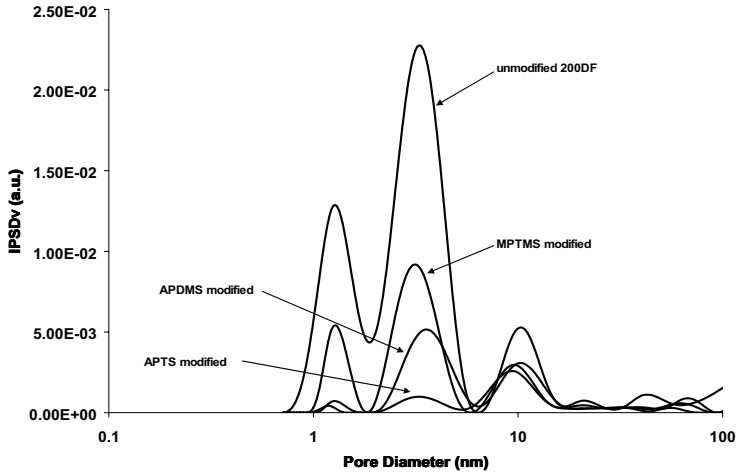

Figure 2. Incremental pore size distributions of 200DF before and after surface modification with APDMS, APTS, and MPTMS.

More significant changes in 200DF porosity are seen as a result of surface modification, since the average pore diameter of this silica gel is much smaller to begin with. Surface modification with 3-mercaptopropyltrimethoxysilane (MPTMS) results in the smallest reduction in porosity, whereas APTS surface modification results in almost complete loss of porosity below 10 nm. This APTS result indicates complete blockage of the smaller pores by APTS, which may explain why less APTS than MPTMS reacts with this silica gel. Note that the smallest diameter 1 nm pores are blocked to an equal extent with APTS or APDMS, but largely remain after MPTMS reaction. The smaller pores, 5 nm or less in diameter, can be blocked by surface polymerization. A second contribution to pore blockage can be from hydrogen bonding interactions between amino groups and residual silanols with APTS and APDMS, while these hydrogen bonding interactions do not occur with MPTMS thiol groups and residual silanols. This may explain why the smallest diameter pores remain to a much larger extent with MPTMS surface modification.

Adsorption isotherms for Cu^{2+} on APTS-modified silicas are shown in Figure 4, and for APDMS-modified silicas in Figure 5. These data show that HP39 > Cab-O-Sil > 200DF with respect to total Cu^{2+} adsorption capacity. Note that more APTS is bonded to 200DF than Cab-O-Sil (Table 1), indicating that a substantial portion of APTS is unavailable for adsorption on 200DF probably because of inaccessibility inside blocked pores. HP39, with the larger pore size, shows the greatest accessibility of Cu^{2+} adsorption with bonded APTS.

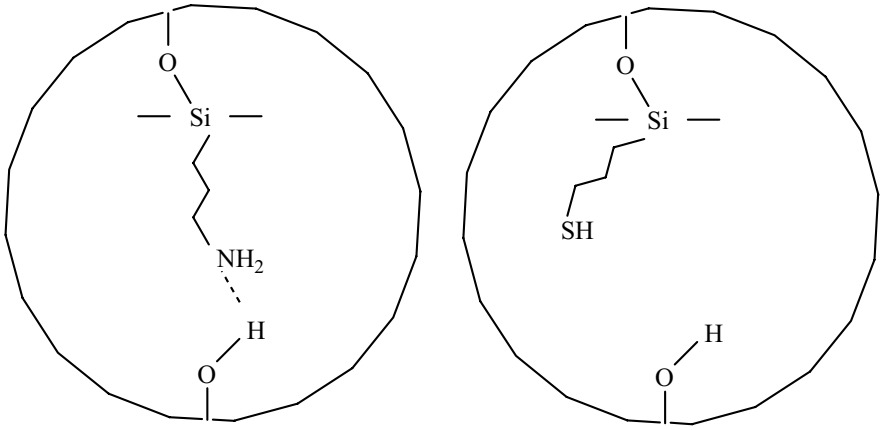

Figure 3. Depiction of hydrogen bonding of an aminosilane with an unreacted silanol inside a small pore (left). Hydrogen bonding is not possible between a mercaptosilane and a residual silanol (right).

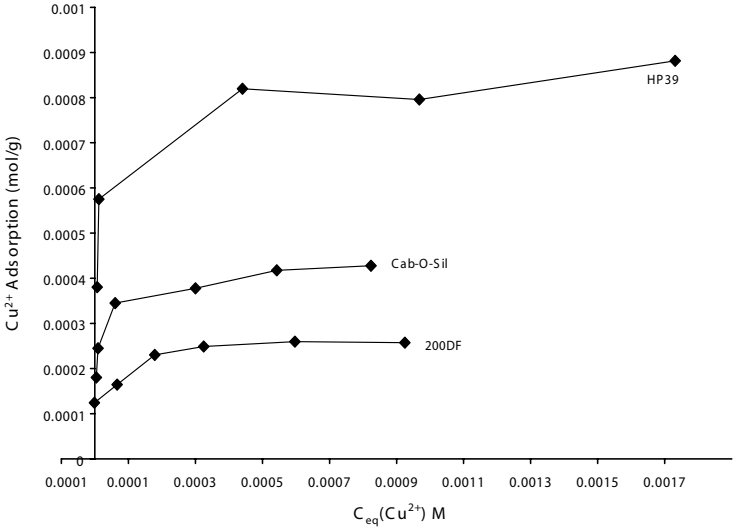

Figure 4. Cu^{2+} adsorption isotherms of APTS-modified silicas.

For APDMS-modified silicas 200DF has at least as large a Cu(II) adsorption capacity as Cab-O-Sil. This is consistent with results in Figures 1 and 2, showing that for APDMS-modified silicas significant porosity remains in the 5 nm pore diameter range, permitting greater accessibility to Cu(II) than for APTS-modified 200DF.

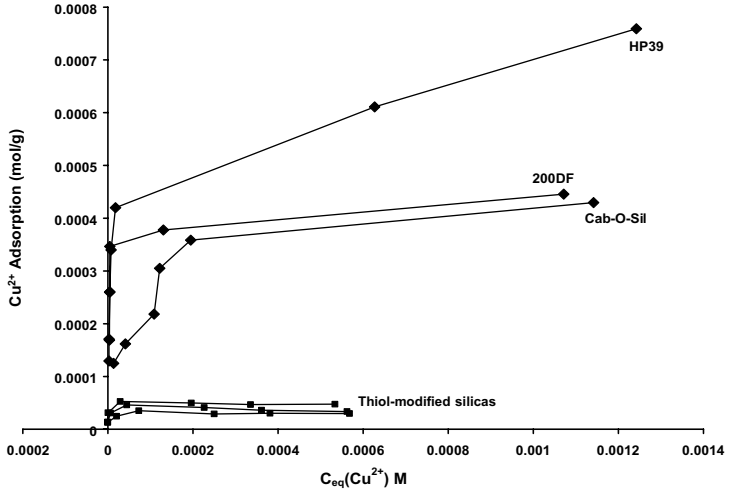

Figure 5. Cu^{2+} adsorption isotherms of APDMS and thiol-modified silicas.

Adsorption free energy distribution functions can be calculated from the ion adsorption isotherms. Figure 6 shows a plot of this data for Cu(II) adsorption on APDMS-modified silicas.

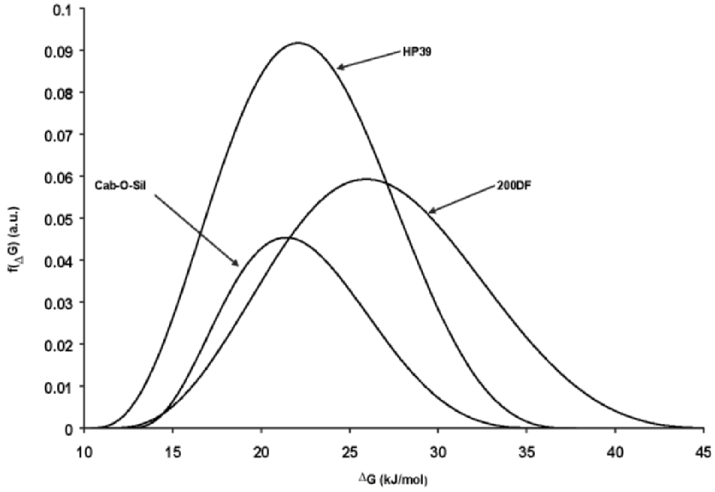

Figure 6. Distribution function of changes in Gibbs free energy of Cu(II) adsorption on APDMS silicas.

The shift to greater negative Gibbs free energy of Cu(II) adsorption on APDMS modified 200DF silica is readily apparent. This trend does not hold for APTS-modified silicas (not shown). The presence of small mesopores in APDMS-modified 200DF silica gel may favor the free energy of adsorption (Figure 2). These types of pores are not present after APTS surface modification (Figure 1), resulting in no enhancement of $-\Delta G_{ads}$. It would thus appear that a compromise must be struck between a favorable free energy of adsorption promoted by small mesopores on 200DF, and enhanced accessibility to surface adsorption sites inside larger mesopores on HP39.

Data in Figure 5 illustrates the large differences in Cu(II) adsorption capacity for thiol- and amino-modified silicas, the former being much less than the latter. It is interesting to note that calculated adsorption free energies for Cu(II) on amino- and thiol-modified silicas are similar, even though their adsorption capacities are quite a bit different.

The large differences seen in Cu(II) adsorption capacity for thiol- and amino-modified silicas does not occur for Pb(II) adsorption (Figure 7). While it is tempting to argue these differences in adsorption behavior based on hard-soft acid-base theory the hardness of Cu^{2+} and Pb^{2+} are very similar, both generally categorized as intermediate cases.[18] It is more likely that Pb(II) adsorption behavior under the conditions of this study is dictated largely by solution behavior and speciation of Pb^{2+} in aqueous solution at pH 5. Indeed it was found that these solutions were unstable and prone to precipitation slowly over time under these conditions. Further work will be needed as a function of pH, surface functionality, and metal ion to determine the role of various factors on adsorption behavior of these systems.

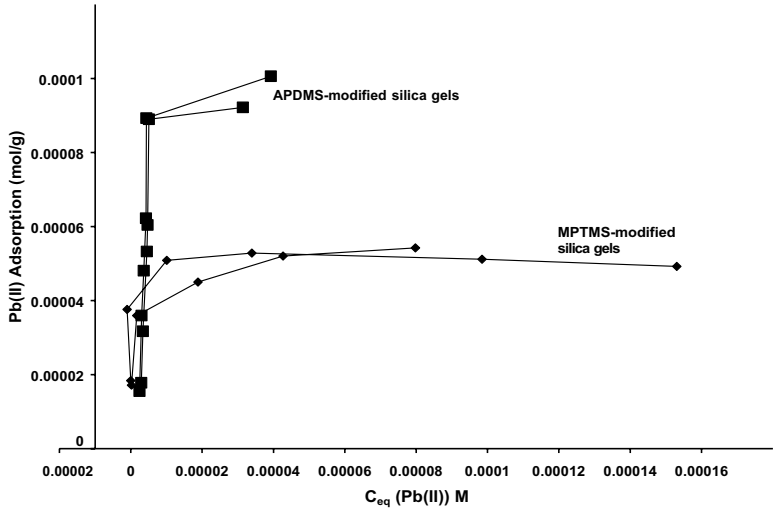

Figure 7. Pb(II) adsorption isotherms on 3-aminopropyldimethylmethoxysilane (APDMS) modified silica gels, and 3-mercaptopropyltrimethoxysilane (MPTMS) modified silica gels.

4. Conclusion

Surface functionalization of high surface area silicas with Lewis bases for the coordination of metal cations, is an effective means to rid aqueous solutions of these unwanted species. Maximum adsorption capacity is achieved using a mesoporous silica with relatively large (~20 nm) pore diameter reacted with a cross-linkable aminopropylsilane. The maximum driving force, measured by ΔG_{ads}, is obtained using a non-crosslinkable aminosilane-modified mesoporous silica with a much smaller average pore diameter (~5 nm after surface modification). This suggests an approach using a silica gel with a relatively large pore diameter which, when modified with functional groups for metal ion adsorption, results in a material with a smaller pore diameter providing both maximum adsorption capacity and large negative ΔG_{ads}.

5. Acknowledgments

We thank Dr. Steve Augustine for collection of the N_2 adsorption data. JPB and VMG thank NATO for funding of the Advanced Research Workshop where this work was presented. This work was supported in part by a grant from the Petroleum Research Fund administered by the American Chemical Society.

References

1. C. Kantipuly, S. Katragadda, A. Chow, and H. D. Gesser, Chelating polymers and related supports for separation and preconcentration of trace metals, *Talanta* 37(5), 491-517 (1990).
2. P. K. Jal, S. Patel, and B. K. Mishra, Chemical modification of silica surface by immobilization of functional groups for extractive concentration of metal ions, *Talanta* 62, 1005-1028 (2004).
3. R. Celis, M. Carmen Hermosin, and J. Cornejo, Heavy metal adsorption by functionalized clays, *Environ. Sci. Technol.* 34, 4593-4599 (2000).
4. L. Mercier and T. J. Pinnavaia, A functionalized porous clay heterostructure for heavy metal ion (Hg^{2+}) trapping, *Micropor. Mesopor. Mater.* 20(1-3), 101-106 (1998).
5. K. J. Edler, Current understanding of formation mechanisms in surfactant-templated materials, *Aust. J. Chem.* 58, 627-643 (2004).
6. D. E. Leyden and H. G. Luttrell, Preconcentration of trace metals using chelating groups immobilized via silylation, *Anal. Chem.* 47(9), 1612-1617 (1975).
7. C. Nguyen and D. D. Do, A new method for the characterization of porous materials, *Langmuir* 15(10) 3608-3615 (1999).

8. C. Nguyen and D. D. Do, Effects of probing vapors and temperature on the characterization of micro- and mesopore size distribution of carbonaceous materials, *Langmuir* 16(18), 7218-7222 (2000).
9. V. M. Gun'ko, J. Skubiszewska-Zięba, R. Leboda, K. N. Khomenko, O. A. Kazakova, M. O. Povazhnyak, and I. F. Mironyuk, Influence of morphology and composition of fumed oxides on changes in their structural and adsorptive characteristics on hydrothermal treatment at different temperatures, *J. Colloid Interface Sci.* 269, 403-424 (2004).
10. V. M. Gun'ko, E. F. Voronin, I. F. Mironyuk, R. Leboda, J. Skubiszewska-Zięba, E. M. Pakhlov, N. V. Guzenko, and A. A. Chuiko, The effect of heat, adsorption and mechanochemical treatments on stuck structure and adsorption properties of fumed silicas, *Colloids Surf. A* 218(1-3), 125-135 (2003).
11. V. M. Gun'ko, V. I. Zarko, E. F. Voronin, V. V. Turov, I. F. Mironyuk, I. I. Gerashchenko, E. V. Goncharuk, E. M. Pakhlov, N. V. Guzenko, R. Leboda, J. Skubiszewska-Zięba, W. Janusz, S. Chibowski, Yu. N. Levchuk, and A. V. Klyueva, Impact of some organics on structural and adsorptive characteristics of fumed silica in different media, *Langmuir* 18(3), 581-596 (2002).
12. E. F. Voronin, V. M. Gun'ko, N. V. Guzenko, E. M. Pakhlov, L. V. Nosach, M. L. Malysheva, J. Skubiszewska-Zięba, R. Leboda, M. V. Borysenko, and A. A. Chuiko, Interaction of poly(ethylene oxide) with fumed silica, *J. Colloid Interface Sci.* 279, 326-340 (2004).
13. V. M. Gun'ko, D. J. Sheeran, S. M. Augustine, and J. P. Blitz, Structural and energetic characteristics of silicas modified by organosilicon compounds, *J. Colloid Interface Sci.* 249, 123-133 (2002).
14. V. M. Gun'ko, V. I. Zarko, D. J. Sheeran, J. P. Blitz, R. Leboda, W. Janusz, and S. Chibowski, Characteristics of modified Cab-O-Sil in aqueous media, *J. Colloid Interface Sci.* 252, 109-118 (2002).
15. M. V. Borysenko, V. M. Gun'ko, A. G. Dyachenko, I. Y. Sulim, R. Leboda, and J. Skubiszewska-Zięba, *Appl. Surf. Sci.* 242, 1-12 (2005).
16. V. M. Gun'ko, I. F. Mironyuk, V. I. Zarko, E. F. Voronin, V. V. Turov, E. M. Pakhlov, E. V. Goncharuk, Yu. M. Nicheporuk, T. V. Kulik, B. B. Palyanytsya, S. V. Pakhovchishin, N. N. Vlasova, P. P. Gorbik, O. A. Mishchuk, A. A. Chuiko, J. Skubiszewska-Zięba, W. Janusz, A. V. Turov, and R. Leboda, Morphology and surface properties of fumed silicas, *J. Colloid Interface Sci.* 289, 427-445 (2005).
17. S. W. Provencher, A constrained regularization method for inverting data represented by linear algebraic or integral equations, *Comp. Phys. Comm.* 27, 213-227 (1982).
18. G. L. Miessler and D. A. Tarr, *Inorganic Chemistry, 2nd Edition* (Prentice-Hall, New Jersey, 1998).